

# SCIENTIFIC REPORTS



OPEN

## Layered polymeric nitrogen in $\text{RbN}_3$ at high pressures

Xiaoli Wang<sup>1,2</sup>, Jianfu Li<sup>3</sup>, Ning Xu<sup>4</sup>, Hongyang Zhu<sup>5</sup>, Ziyu Hu<sup>2</sup> & Li Chen<sup>1</sup>

Received: 05 August 2015

Accepted: 14 October 2015

Published: 13 November 2015

The structural evolutionary behaviors of nitrogen in  $\text{RbN}_3$  have been studied up to 300 GPa using a particle swarm optimization structure searching method combined with density functional calculations. Three stable new phases with *P*-1, *P6/mmm* and *C2/m* structure at pressure of 30, 50 and 200 GPa are identified for the first time. The analysis of the crystal structures of three new predicted phases reveals that the transition of  $\text{N}_3^-$  ions goes from linear molecules to polymeric chains, benzene-like rings and then to polymeric layers induced by pressure. The electronic structures of three predicted phases reveal that the structural changes are accompanied and driven by the change of orbital hybridization of N atoms from *sp* to *sp*<sup>2</sup> and finally to partial *sp*<sup>3</sup>. Most interestingly, the Rb atoms show obvious transition metal-like properties through the occupation of 4*d* orbitals in high-pressure phases. Moreover, the Rb atoms are characterized by strong hybridization between 4*d* orbitals of Rb and 2*p* orbitals of N in *C2/m* structure. Our studies complete the structural evolution of  $\text{RbN}_3$  under pressure and reveal for the first time that the Rb atoms in rubidium nitride possess transition element-like properties under pressure.

Metal azides have been the subjects of many studies including their structural stability, lattice dynamics, electronic structure, and many other physical properties because of their linear azide anion<sup>1</sup>, as well as their significant industrial importance as gas generators and explosives<sup>2</sup>. Recently, taking metal azides as starting materials to synthesis polymeric nitrogen, a potential high-energy-density-material, has become a new topic due to the potential lower synthesis pressure compared with pure nitrogen gas. In nitrogen gas, nitrogen exists in  $\text{N}_2$  molecules and the connection between nitrogen atoms is triple bonds  $\text{N}\equiv\text{N}$ . In metal azides, nitrogen exists in  $\text{N}_3^-$  anions and the nitrogen atoms are connected through double bonds  $\text{N}=\text{N}$ . It is expected that the  $\text{N}_3^-$  anions in metal azides may form a polymeric nitrogen network more readily than  $\text{N}_2$  molecules, since the  $\text{N}=\text{N}$  have a much lower bonding energy (418 KJ/mol) than the  $\text{N}\equiv\text{N}$  (954 KJ/mol). Under pressure,  $\text{N}_3^-$  anion will undergo a series of structural transitions accompanied by the change of hybridization type of nitrogen atoms, as shown in Fig. 1. Under low pressure, usually fewer than 30 GPa,  $\text{N}_3^-$  anions maintains their linear structures with *sp* hybridization, in which the crystal maybe undergo orientational phase transition of  $\text{N}_3^-$  anions induced by pressure<sup>3–7</sup>. As pressure increase,  $\text{N}_3^-$  anions translates to a so called pseudo-benzene  $\text{N}_6$  ring with *sp*<sup>2</sup> hybridization<sup>4,5,8,9</sup>. Continuing to increase pressure, nitrogen will form polymeric structure with partial *sp*<sup>3</sup> hybridization. For  $\text{CsN}_3$ , our previous work indicates that  $\text{N}_3^-$  anions will translate to a chain like structure at 51 GPa instead of  $\text{N}_6$  ring<sup>10</sup>. In the process of nitrogen structural transition, alkali metal atoms in azides act as electronic donors to change the connection between nitrogen atoms and electronic properties of compounds. A lot of experimental and theoretical work has been done to study the high-pressure behaviors of nitrogen in  $\text{LiN}_3$ <sup>4,8,11–15</sup>,  $\text{NaN}_3$ <sup>3,5,16</sup>,  $\text{KN}_3$ <sup>7,9,14,17–21</sup>, and  $\text{CsN}_3$ <sup>10,22</sup>. Therefore, a study of the high-pressure behavior of  $\text{RbN}_3$  would provide more insights into the mechanism of pressure-induced structural

<sup>1</sup>Institute of Condensed Matter Physics, Linyi University, Linyi 276005, P. R. China. <sup>2</sup>Beijing Computational Science Research Center, Beijing, 100084, P. R. China. <sup>3</sup>School of science, Linyi University, Linyi 276005, P. R. China. <sup>4</sup>Department of Physics, Yancheng Institute of Technology, Yancheng 224051, China. <sup>5</sup>State Key Laboratory of Superhard Materials, College of Physics, Jilin University, Changchun 130012, P. R. China. Correspondence and requests for materials should be addressed to J.L. (lijianfu@lyu.edu.cn)

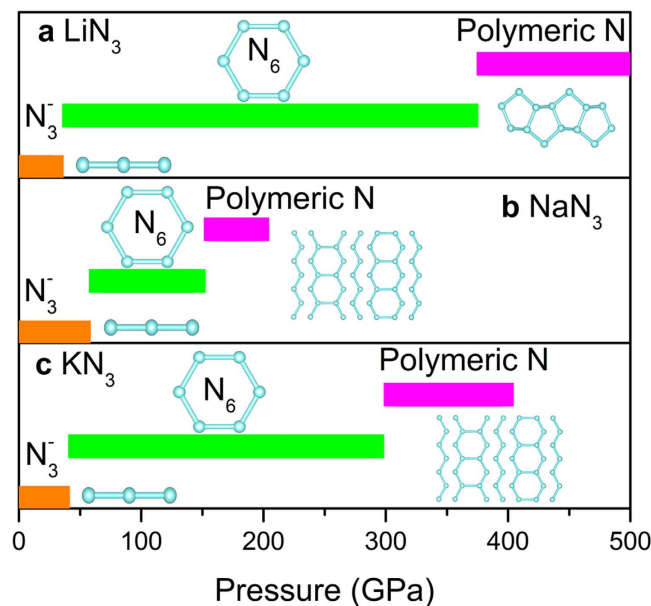


**Figure 1.** Structural evolution of  $N_3^-$  anion in alkali metal azides under compression. (a)  $LiN_3$ , (b)  $NaN_3$ , and (c)  $KN_3$ . Transition pressure and structures are taken from reference  $LiN_3^4$ ,  $NaN_3^5$ , and  $KN_3^7$ , respectively.

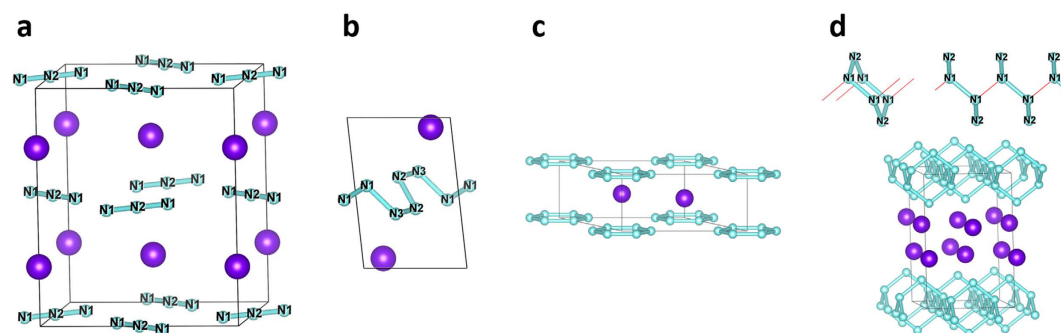


**Figure 2.** Crystal structures. The ambient condition and the predicted high-pressure phase: (a)  $I4/mcm$ ; (b)  $P-1$ ; (c)  $P6/mmm$ ; and (d)  $C2/m$ . The large and small spheres denote rubidium and nitrogen atoms, respectively. The red lines denote the connection between  $N_6$  rings in up section of (d). The nitrogen atoms in (a,b,d) have been labeled N1, N2, and N3 according to their Wyckoff positions.

evolution of  $N_3^-$  anions. It is helpful to investigate theoretically the pressure effect on rubidium azide and the role of rubidium atoms in the structural evolution process of  $N_3^-$  anions.

Under ambient conditions,  $\alpha$ - $RbN_3$  has the lowest energy with a body-centered tetragonal (bct) lattice of space group  $I4/mcm$ , in which rubidium (Rb), nitrogen 1 (N1), and nitrogen 2 (N2) atoms are located on the 4a,4d, and 8h Wyckoff positions, respectively (Fig. 2a), which is isostructural to the low-temperature phase of  $KN_3$  and  $CsN_3$  in all respects<sup>23</sup>. The nitrogen, linear and symmetric, occupy alternately  $[0,1,1]$  and  $[1\bar{1}0]$  directed position in the crystal forming planes ( $(0\ 0\ 1)$  and  $(0\ 0\ 2)$  planes) separated by layers of Rb ions. Recently, for the high-pressure behaviors of  $RbN_3$ , we present the *in-situ* X-ray diffraction studies of  $RbN_3$  up to 42.0 GPa at room temperature<sup>6</sup>. Two pressure-induced orientational phase transitions of  $\alpha$ - $RbN_3$  ( $I4/mcm$ )  $\rightarrow$   $\gamma$ - $RbN_3$  ( $C2/m$ )  $\rightarrow$   $\delta$ - $RbN_3$  were identified at 6.5 and 16.0 GPa, respectively.

In this work, we will focus on the structural evolution of anions under high pressure. A series of phase transitions in which  $N_3^-$  is converted to a chain like structure  $N_6$  ring and layered polymeric nitrogen have been discovered up to 300 GPa by using a specifically developed particle swarm optimization (PSO) algorithm technique for crystal structure prediction<sup>24</sup>. To confirm the thermal dynamic stabilities of new phases, phonon dispersion spectroscopies have been calculated. The electronic properties calculations indicate the  $4d$  orbitals of Rb have been partially occupied in high-pressure phases and a strong hybridization has been formed between  $4d$  orbital of Rb and  $2p$  orbital of N in layered structure of  $RbN_3$ .

Space group	Pressure (GPa)	Lattice parameters (Å, °)		Atom	Wyckoff positions	x	y	z
<i>I4/mcm</i>	0	a = 6.2871 (6.3098)	$\alpha = 90$	Rb	4a	0	0	0.25
		b = 6.2871 (6.3098)	$\beta = 90$	N1	8h	0.3664	0.1336	0
		c = 7.5106 (7.5188)	$\gamma = 90$	N2	4d	0.5	0	0
<i>P-1</i>	40	a = 3.3263	$\alpha = 96.7544$	Rb	2i	0.8007	0.9350	0.7555
		b = 4.7467	$\beta = 75.1448$	N1	2i	0.1171	0.5467	0.8935
		c = 5.5230	$\gamma = 97.8611$	N2	2i	0.4330	0.6051	0.4513
				N3	2i	0.6319	0.6399	0.2184
<i>P6/mmm</i>	100	a = 5.5482	$\alpha = 90$	Rb	2d	0.3333	0.6667	0.5
		b = 5.5482	$\beta = 90$	N	6j	0.7684	0.7684	0
		c = 5.5482	$\gamma = 120$					
<i>C2/m</i>	300	a = 3.9946	$\alpha = 90$	Rb	4i	0.2234	0	0.3843
		b = 4.0911	$\beta = 98.6538$	N1	8j	0.8612	0.2517	0.9327
		c = 6.1675	$\gamma = 90$	N2	4i	0.8201	0.5	0.8029

**Table 1.** The unit-cell parameters and atomic positions of the *I4/mcm*, *P-1*, *P6/mmm* and *C2/m* phase at 0 GPa, 40 GPa, 100 GPa and 300 GPa, respectively.

## Computational Details

We have performed extensive structure searches to uncover the high-pressure structures of  $\text{RbN}_3$  based on a global minimization of free-energy surfaces merging *ab initio* total energy calculations via PSO technique, as implemented in the Crystal Structure Analysis by Particle Swarm Optimization (CALYPSO) code<sup>24,25</sup>. This method has successfully predicted the ground state structure for various systems including Nitrogen<sup>26</sup>, Caesium<sup>27</sup>, and superhard carbon nitride<sup>28</sup>. The underlying *ab initio* structural relaxations and electronic band structure calculations are performed in the framework of density functional theory within generalized gradient approximation Perdew-Burke-Ernzerhof (GGA-PBE)<sup>29</sup>, as implemented in the VASP code<sup>30</sup>. The projector augmented wave (PAW)<sup>31</sup> pseudopotentials are adopted with the PAW potentials taken from the VASP library where  $4p^65s^1$  and  $2s^22p^3$  are treated as valence electrons for Rb and N atoms, respectively. The cutoff energy (800 eV) for the expansion of the wave function into plane waves and Monkhorst-Pack<sup>32</sup>  $k$ -meshes ( $k$ -points density  $0.03 \text{ \AA}^{-1}$ ) are chosen to ensure that all the enthalpy calculations are well converged to better than 1 meV/atom. The calculations of net charge are based on Bader analysis<sup>33,34</sup>. The phonon calculations are carried out by using a supercell approach as implemented in the PHONOPY code<sup>35</sup>.

## Results and Discussion

The variable-cell high-pressure structure predictions have been performed within a pressure region from 0 to 300 GPa, with system containing from one to eight formula units per simulation cell as implemented in CALYPSO code. Our structural searches identified not only the ambient conditions phase *I4/mcm* shown in Fig. 2a, three new structures are also depicted in Fig. 2b,d. The lattice constants of predicted structure at ambient pressure  $a = 6.2871 \text{ \AA}$  and  $c = 7.5106 \text{ \AA}$  are in agreement with the results obtained in experiment ( $a = 6.3098 \text{ \AA}$  and  $c = 7.5188 \text{ \AA}$ )<sup>23</sup> which validates our computational method adopted here. The  $\text{N}_3^-$  ions are linear and symmetric, and the bond length of  $\text{N}=\text{N}$  is  $1.187 \text{ \AA}$ , which is same as that in potassium azides and well in agreement with the experimental results ( $1.176 \text{ \AA}$ )<sup>23</sup>. The calculated atomic fractional coordinates are summarized in Table 1. The results indicate that  $\text{N}_3^-$  anions undergo transition of  $\text{N}_3^- \rightarrow \text{N}$  chain  $\rightarrow \text{N}_6$  ring  $\rightarrow$  layered N. Different from converting directly into  $\text{N}_6$  ring structure in  $\text{LiN}_3$ <sup>4,8</sup>,  $\text{NaN}_3$ <sup>5</sup>, and  $\text{KN}_3$ <sup>7,9</sup>,  $\text{N}_3^-$  anions translate to chain-like structure, which appears in  $\text{CsN}_3$ <sup>10</sup> at 51 GPa, before entering  $\text{N}_6$  ring structure. The layered nitrogen in *C2/m* phase is constructed by chair-like  $\text{N}_6$  rings, as shown in up section of Fig. 2d, completely different from the high-pressure structures in  $\text{LiN}_3$ <sup>4</sup>,  $\text{NaN}_3$ <sup>5</sup>, and  $\text{KN}_3$ <sup>7</sup>. In *C2/m* phase, nitrogen atoms have two nonequivalent sites 8j and 4i, respectively. The nitrogen atom located on 8j site is connected with three neighboring N through three N-N bonds and the N located on 4i site is connected with two neighboring N through two N-N bonds.

To investigate the energetic stabilities of  $\text{RbN}_3$  compound under high pressure, we calculate the formation enthalpy relative to the *I4/mcm* structure of  $\text{RbN}_3$  in a pressure range from 0 to 300 GPa, as shown in Fig. 3a. The most stable structure is a tetragonal phase with *I4/mcm* symmetry from ambient pressure which is then replaced by a lower-enthalpy *P-1* structure at 30 GPa. Above 50 GPa, a hexagonal structure with *P6/mmm* symmetry is favored over other structures and remains the lowest-enthalpy

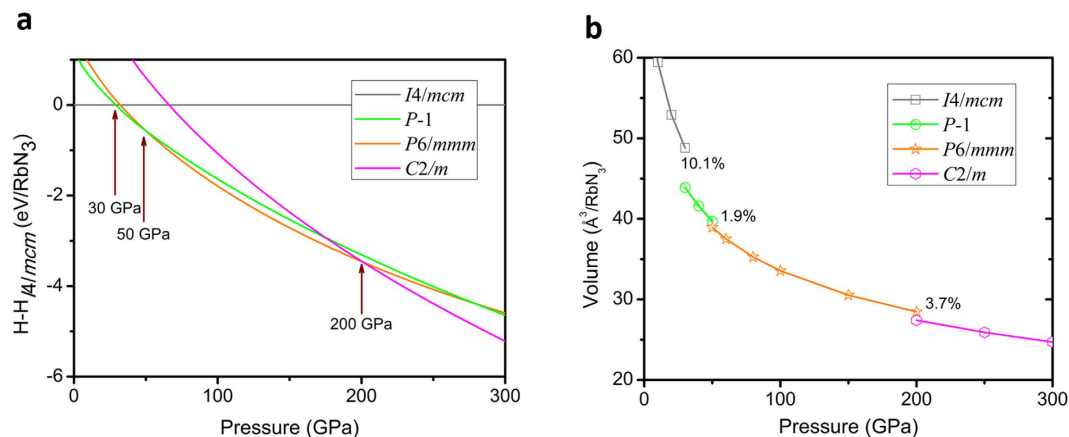


**Figure 3.** (a) Enthalpy of formation of selected structures of RbN<sub>3</sub> as a function of pressure (relative to the *I4/mcm* phase). (b) Phase diagram of RbN<sub>3</sub> at pressure region from 0 to 300 GPa.

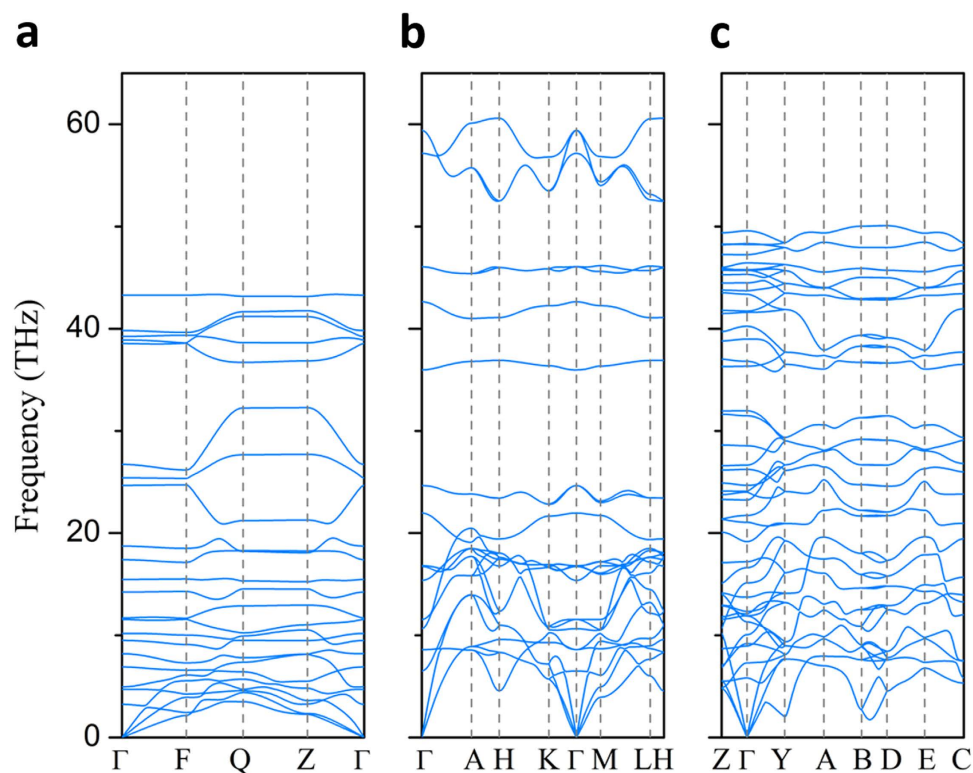


**Figure 4.** Phonon-dispersion curves of predicted structures. (a) *P-1*, (b) *P6/mmm*, and (c) *C2/m* at 40 GPa, 100 GPa and 300 GPa, respectively.

phase up to 200 GPa. Continuously increasing pressure, the RbN<sub>3</sub> will translate to a monoclinic structure with *C2/m* symmetry. Thorough structure searches using CALYPSO do not find any other structural change up to 300 GPa. The fact that the four structures are in entirely different crystal symmetry suggests that the transitions between them are first order which is indeed confirmed by the calculated P-V curves (Fig. 3b). The reductions of the volumes are found to be 10.1%, 1.9% and 3.7% for the transitions from *I4/mcm* to *P-1*, from *P-1* to *P6/mmm* and from *P6/mmm* to *C2/m*, respectively.

The dynamic stability of three predicted structures are examined by calculating the phonon spectra using the supercell method<sup>35</sup>. No imaginary phonon frequency is found in the whole Brillouin zone at the pressure 40 GPa, 100 GPa and 300 GPa, respectively, as shown in Fig. 4.

Under pressure, the structural evolution of the rubidium azide is accompanied by the change of the electronic properties. To explore that, we calculated the electronic structures and their dependence on

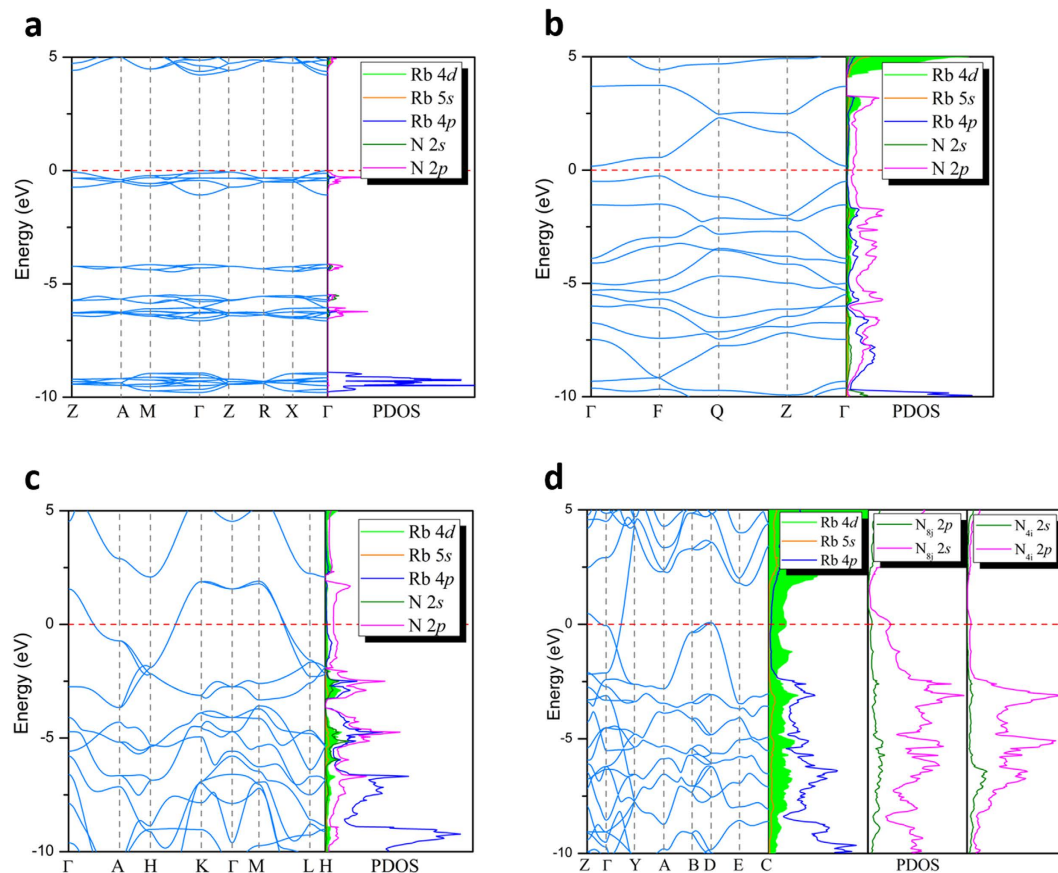


**Figure 5.** Band structure and projected density of states. (a)  $I4/mcm$ , (b)  $P-1$ , (c)  $P6/mmm$ , and (d)  $C2/m$  at 0 GPa, 40 GPa, 100 GPa and 300 GPa, respectively. Dash line denotes Fermi energy level.

pressure in several aspects, including the electron localized functions (ELF), band structures, electronic band structure, projected density of states (PDOS), and net charge of Rb atoms.

As shown in Fig. 5, the four phase transitions of  $RbN_3$  are accompanied by insulator-metal-metal transitions. At ambient conditions, the  $I4/mcm$  structure is an insulator characterized by a large energy gap of 4.3 eV that is similar to the atmospheric pressure phases of other alkali metal azides<sup>7,10,12</sup>. However, the  $P-1$ ,  $P6/mmm$  and  $C2/m$  structures exhibit clear metallic behaviors by evidence of cross of band structures and the finite electronic DOS at the Fermi level. As can be seen from the partial DOS,  $N-2p$  states contribute most to the valence band and the DOS near the Fermi level in  $P-1$  and  $P6/mmm$  structures. The detailed analysis for metallicity of  $P-1$  and  $P6/mmm$  can be found in previous works for  $CsN_3$ <sup>10</sup> and  $KN_3$ <sup>7,9</sup> due the similar electronic properties. For four considered structures, the strong covalent bonding between nitrogen atoms as well as the lone pairs electrons are revealed clearly by the ELF shown in Fig. 6. As pressure increase, the hybridization type between nitrogen atoms undergoes from  $sp$  (within  $I4/mcm$ ) to  $sp^2$  (within  $P-1$  and  $P6/mmm$ ), then to partial  $sp^3$  (within  $C2/m$ ).

More interestingly, the  $4d$  orbital of rubidium is partially occupied in high-pressure phases as shown in Fig. 5b,d and there is an obvious orbital hybridization between the  $4d$  of Rb and  $2p$  of N located on 8j sites in  $C2/m$  phase. To further confirm this result, we recalculate the PDOS of the four phases using a much small Wigner-Seitz radius, in which we change the spherical radius from defaults value in pseudo-potential (2.418 and 0.741 Å for Rb and N) to smaller values based on the Bader analysis, as shown in supplementary Figure S1-S3. The recalculated results are similar to the previous PDOS for the four phases except the value of densities. To study the impact of partial occupation of  $4d$  orbital on electronic properties, we calculate the net charge of Rb atom based on Bader analysis, as shown in Fig. 7. At ambient conditions, the Rb atoms contribute almost one electron (0.85) to three N atoms forming  $N_3^-$  anion.

Under high pressure, the net charge decreases due to the partial occupation of  $5d$  orbital, though the Rb atom still loses its  $5s$  electron. Though the transition metal-like property of Rb elements has been reported by both experimental and theoretical works in alkali metal elements under high pressure<sup>36-38</sup>, there has been no research addressing that in chemical compounds. The difference that comes from the

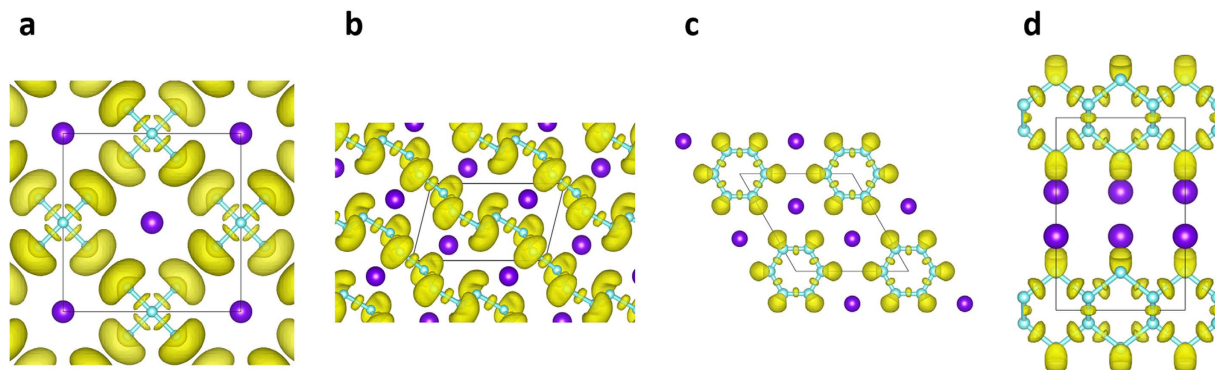


**Figure 6. The electron localized functions.** (a)  $I4/mcm$ , (b)  $P-1$ , (c)  $P6/mmm$ , and (d)  $C2/m$  at 0 GPa, 40 GPa, 100 GPa and 300 GPa, respectively. The value of isosurface is 0.8.

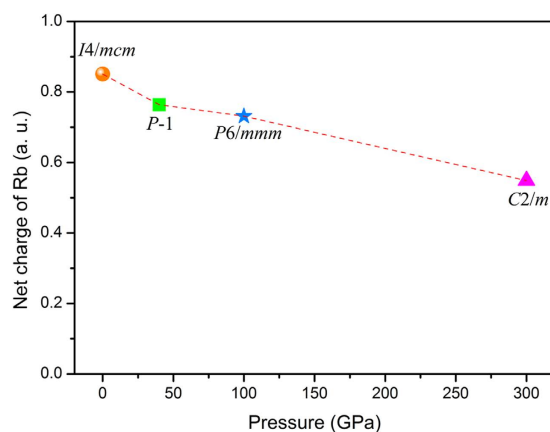


**Figure 7. The net charge of Rb atoms based on Bader charge analysis for Rb in  $I4/mcm$ ,  $P-1$ ,  $P6/mmm$  and  $C2/m$  phases at 0 GPa, 40 GPa, 100 GPa and 300 GPa, respectively.**

occupation of  $d$  orbitals is caused by the  $spd$  hybridization in alkali metal elements, for  $RbN_3$  that results from the hybridization between  $4d$  of Rb and  $2p$  of N which may enhance the stability of compound.

## Conclusion

In summary, we studied the evolution of the structures of  $RN_3$  under high pressure by using an unbiased automatic structure search method based on first-principles total energy calculations and geometry optimization. We predicted three new high-pressure structures of  $RbN_3$  with  $P-1$ ,  $P6/mmm$  and  $C2/m$  structure at pressure of 30, 50 and 200 GPa. This result extends the high-pressure structures  $RbN_3$ . The analysis of the electronic structure reveals that the transition trend of  $N_3^-$  ions from linear molecules to polymer chains, then to benzene-like rings, and finally to layered polymeric nitrogen is driven by the hybridization of N atoms in which the nitrogen hybridized types are  $sp$ ,  $sp^2$ ,  $sp^2$ , and partial  $sp^3$ , respectively. For the first time, we reveal that the Rb atoms in  $RbN_3$  possess obvious transition metal-like properties under high pressure. In  $C2/m$  phase, a strong hybridization has been found between  $4d$  orbitals of Rb and  $2p$  orbitals of N.

## References

- Fuith, A. The KSCN family: Structural properties and phase transitions of crystals with three-atomic linear anions. *Phase Transitions A Multimat. J.* **62**, 1–93 (1997).
- Evans, B. L., Yoffe, A. D. & Gray, P. Physics and chemistry of the inorganic azides. *Chem. Rev.* **59**, 515–564 (1959).
- Zhu, H. *et al.* Pressure-induced series of phase transitions in sodium azide. *J. Appl. Phys.* **113**, 033511 (2013).
- Wang, X. *et al.* Polymerization of nitrogen in lithium azide. *J. Chem. Phys.* **139**, 1–6 (2013).
- Zhang, M. *et al.* Structural and electronic properties of sodium azide at high pressure: A first principles study. *Solid State Commun.* **161**, 13–18 (2013).
- Li, D. *et al.* Pressure-induced phase transitions in rubidium azide: Studied by *in-situ* x-ray diffraction. *Appl. Phys. Lett.* **105**, 071903 (2014).
- Li, J. *et al.* Pressure-induced polymerization of nitrogen in potassium azides. *EPL (Europhysics Lett.)* **104**, 16005 (2013).

8. Zhang, M., Yan, H., Wei, Q., Wang, H. & Wu, Z. Novel high-pressure phase with pseudo-benzene 'N<sub>6</sub>' molecule of LiN<sub>3</sub>. *EPL (Europhysics Lett.)* **101**, 26004 (2013).
9. Zhang, J. & Zeng, Z., Lin, H.-Q. & Li, Y.-L. Pressure-induced planar N<sub>6</sub> rings in potassium azide. *Sci. Rep.* **4**, 4358 (2014).
10. Wang, X., Li, J., Zhu, H., Chen, L. & Lin, H. Polymerization of nitrogen in cesium azide under modest pressure. *J. Chem. Phys.* **141**, 044717 (2014).
11. Medvedev, S. *et al.* Phase stability of lithium azide at pressures up to 60 GPa. *J. Physics. Condens. Matter* **21**, 195404 (2009).
12. Babu, K. R., Lingam, C. B., Tewari, S. P. & Vaitheeswaran, G. High-pressure study of lithium azide from density-functional calculations. *J. Phys. Chem. A* **115**, 4521–9 (2011).
13. Huang, X. *et al.* Large volume collapse during pressure-induced phase transition in lithium amide. *J. Phys. Chem. C* **116**, 9744–9749 (2012).
14. Ramesh Babu, K., Vaitheeswaran, G. & Babu, K. R. Metal azides under pressure: An emerging class of high energy density materials. *J. Chem. Sci.* **124**, 1391–1398 (2012).
15. Prasad, D. L. V. K., Ashcroft, N. W. & Hoffmann, R. Evolving Structural Diversity and Metallicity in Compressed Lithium Azide. *J. Phys. Chem. C* **117**, 20838 (2013).
16. Eremets, M. I. *et al.* Polymerization of nitrogen in sodium azide. *J. Chem. Phys.* **120**, 10618–23 (2004).
17. Ji, C. *et al.* High pressure X-ray diffraction study of potassium azide. *J. Phys. Chem. Solids* **72**, 736–739 (2011).
18. Ramesh Babu, K. & Vaitheeswaran, G. Ab-initio study of structural and vibrational properties of KN<sub>3</sub> under pressure. *Chem. Phys. Lett.* **533**, 35–39 (2012).
19. Ji, C. *et al.* Pressure-induced phase transition in potassium azide up to 55 GPa. *J. Appl. Phys.* **111**, 112613 (2012).
20. Hou, D. *et al.* Phase transition and structure of silver azide at high pressure. *J. Appl. Phys.* **110**, 023524 (2011).
21. Hooper, J. & Zurek, E. High Pressure Potassium Polyhydrides: A Chemical Perspective. *J. Phys. Chem. C* **116**, 13322–13328 (2012).
22. Hou, D. *et al.* Series of phase transitions in cesium azide under high pressure studied by *in situ* x-ray diffraction. *Phys. Rev. B* **84**, 064127 (2011).
23. Müller, U. Crystal structure refinements of KN<sub>3</sub>, RbN<sub>3</sub>, CsN<sub>3</sub> and TiN<sub>3</sub>. *Z. Anorg. Allg. Chem.* **392**, 159–166 (1972).
24. Wang, Y., Lv, J., Zhu, L. & Ma, Y. Crystal structure prediction via particle-swarm optimization. *Phys. Rev. B* **82**, 094116 (2010).
25. Wang, Y., Lv, J., Zhu, L. & Ma, Y. CALYPSO: A method for crystal structure prediction. *Comput. Phys. Commun.* **183**, 2063–2070 (2012).
26. Wang, X. *et al.* Cagelike Diamondoid Nitrogen at High Pressures. *Phys. Rev. Lett.* **109**, 175502 (2012).
27. Miao, M.-S. Caesium in high oxidation states and as a *p*-block element. *Nat. Chem.* **5**, 846–852 (2013).
28. Wang, X., Bao, K., Tian, F. & Meng, X. Cubic gauche-CN: A superhard metallic compound predicted via first-principles calculations. *J. Chem. Phys.* **133**, 044512 (2010).
29. Perdew, J., Burke, K. & Ernzerhof, M. Generalized Gradient Approximation Made Simple. *Phys. Rev. Lett.* **77**, 3865–3868 (1996).
30. Kresse, G. & Furthmüller, J. Efficient iterative schemes for ab initio total-energy calculations using a plane-wave basis set. *Phys. Rev. B* **54**, 11169–11186 (1996).
31. Blöchl, P. Projector augmented-wave method. *Phys. Rev. B* **50**, 17953–17979 (1994).
32. Monkhorst, H. J. & Pack, J. D. Special points for Brillouin-zone integrations. *Phys. Rev. A* **13**, 5188–5192 (1976).
33. Henkelman, G., Arnaldsson, A. & Jónsson, H. A fast and robust algorithm for Bader decomposition of charge density. *Comput. Mater. Sci.* **36**, 354–360 (2006).
34. Tang, W., Sanville, E. & Henkelman, G. A grid-based Bader analysis algorithm without lattice bias. *J. Phys. Condens. Matter* **21**, 084204 (2009).
35. The program Phonopy is available at <http://phonopy.sourceforge.net/>; the force constant matrix is determined by VASP.
36. Parker, L. J., Atou, T. & Badding, J. V. Transition Element-Like Chemistry for Potassium Under Pressure. *Science*. **273**, 95–97 (1996).
37. Ma, Y., Oganov, A. R. & Xie, Y. High-pressure structures of lithium, potassium, and rubidium predicted by an ab initio evolutionary algorithm. *Phys. Rev. B* **78**, 1–5 (2008).
38. Fabbri, G., Lim, J., Veiga, L. S. I., Haskel, D. & Schilling, J. S. Electronic and structural ground state of heavy alkali metals at high pressure. *Phys. Rev. B* **91**, 1–9 (2015).

## Acknowledgements

This work was supported by the National Science Foundation of China under Grants Nos. 11147007, 11304139, 11304111, 11274151, 11404278 and NSAF U1230202, Natural Science Foundation of Shandong Province No. ZR2014JL005, and Key Disciplines of Condensed matter Physics of Linyi University.

## Author Contributions

X.W. and J.L. conceived the research. X.W. carried out the calculations. J.L., X.W., N.X., Z.H., H.Z. and L.C. analyzed the data. X.W. and J.L. wrote the paper.

## Additional Information

**Supplementary information** accompanies this paper at <http://www.nature.com/srep>

**Competing financial interests:** The authors declare no competing financial interests.

**How to cite this article:** Wang, X. *et al.* Layered polymeric nitrogen in RbN<sub>3</sub> at high pressures. *Sci. Rep.* **5**, 16677; doi: 10.1038/srep16677 (2015).



This work is licensed under a Creative Commons Attribution 4.0 International License. The images or other third party material in this article are included in the article's Creative Commons license, unless indicated otherwise in the credit line; if the material is not included under the Creative Commons license, users will need to obtain permission from the license holder to reproduce the material. To view a copy of this license, visit <http://creativecommons.org/licenses/by/4.0/>